

Rhododendrol, a reductive metabolite of raspberry ketone, suppresses the differentiation of 3T3-L1 cells into adipocytes

NAOTO URAMARU, AZUSA KAWASHIMA, MAKOTO OSABE and TOSHIYUKI HIGUCHI

Division of Pharmaceutical Health Biosciences, Nihon Pharmaceutical University, Saitama 362-0806, Japan

Received March 25, 2022; Accepted December 21, 2022

DOI: 10.3892/mmr.2023.12938

Abstract. Obesity is a serious medical condition worldwide, and a major risk factor for type 2 diabetes, metabolic syndrome, cancer and cardiovascular disease. In addition to changes in dietary habits and physical activity, consuming supplements to maintain good health and prevent obesity is important in modern society. Raspberry ketone (RK) is a natural phenolic ketone found in the European red raspberry (*Rubus idaeus* L.) and is hypothesized to prevent obesity when administered orally. The present study found that RK was reduced to rhododendrol (ROH) in human liver microsomes and cytosol. The present study investigated whether the metabolite ROH had anti-adipogenic effects using mouse 3T3-L1 cells. The effects of ROH or RK on lipid accumulation during differentiation of 3T3-L1 pre-adipocyte into adipocyte were determined using Oil Red O staining. CCAAT enhancer-binding protein α (C/EBP α) and peroxisome proliferator-activated receptor γ (PPAR γ) mRNA and protein expression were examined using reverse transcription-quantitative PCR and western blotting analysis, respectively. The present study revealed that ROH suppressed lipid accumulation in the cells, similar to RK. In addition, ROH suppressed the mRNA expression levels of C/EBP α and PPAR γ in 3T3-L1 adipocytes. Furthermore, ROH suppressed PPAR γ protein expression in 3T3-L1 adipocytes. These findings suggested that ROH is an active metabolite with an anti-adipogenic effect, which may contribute to the anti-obesity effect of orally administered RK. The present study indicated that it is important to understand the biological activity of the metabolites of orally administered compounds.

Introduction

Obesity is a major risk factor for type 2 diabetes, metabolic syndrome, cancer, and cardiovascular diseases (1-3). At the cellular level, obesity is characterized by an increase in the number and size of adipocytes differentiated from pre-adipocytes in adipose tissues. In addition, adipose tissues regulate energy homeostasis. An excessive accumulation of adipose tissue results from increased adipogenesis and adipocyte differentiation, leading to the conversion of pre-adipocytes into adipocytes. Adipogenesis and the differentiation of pre-adipocytes into adipocytes are regulated by the expression and/or activation of adipogenesis/lipolysis-related factors (4,5). These pre-adipocytes are used to study the molecular mechanisms of adipogenesis and lipogenesis. Mouse fibroblast 3T3-L1 cells are an established model for obesity research (6). Many studies using 3T3-L1 cells have demonstrated that various compounds suppress cell differentiation into adipocytes and downregulate CCAAT enhancer-binding protein α (C/EBP α) and peroxisome proliferator-activated receptor γ (PPAR γ). The action of these adipogenesis-related factors during the differentiation of 3T3-L1 cells into adipocytes results in the suppression of lipid droplet accumulation in these cells (7,8).

Raspberry ketone (4-(4-hydroxyphenyl)-2-butanone; RK) is one of the major natural phenolic ketone compounds present in European red raspberry (*Rubus idaeus* L.) (9,10), and may possess lipolytic and anti-obesity effects (Fig. 1). Several studies in mice have reported that RK prevents increases in body weight and the weight of the liver and visceral adipose tissues (epididymal, retroperitoneal, and mesenteric) induced by a high-fat diet (11-13). Rhododendrol (4-(4-hydroxyphenyl)-2-butanol; ROH) is present in *Betula platyphylla* and *Acer nikoense* Maximowicz (14,15). When administered orally to mammals, RK is metabolized via several pathways (16). ROH, formed by the reduction of the ketone group of RK, is excreted as a major metabolite after a single oral administration in rats, guinea pigs, and rabbits (17), suggesting that RK is reductively metabolized in the small intestine or liver (first-pass effect) (Fig. 1).

Carbonyl compounds, such as aldehydes and ketones, are converted into their corresponding alcohol metabolites *in vivo*. Interestingly, many xenobiotic carbonyl compounds are metabolized into active reductive metabolites. For example, loxoprofen sodium, an anti-inflammatory drug, is reduced to its active metabolite (18). Sennoside, a natural product, is reduced

Correspondence to: Professor Toshiyuki Higuchi, Division of Pharmaceutical Health Biosciences, Nihon Pharmaceutical University, 10281 Komuro, Ina-machi, Kitaadachi-gun, Saitama 362-0806, Japan
E-mail: higuchi@nichiyaku.ac.jp

Abbreviations: RK, raspberry ketone; ROH, rhododendrol

Key words: rhododendrol, raspberry ketone, metabolic activation, adipocyte, 3T3-L1 cells

to rhein anthrone, an active metabolite produced by intestinal bacteria in mice (19). We also found that ketone-containing medicines, such as metyrapone, acetohexamide, and befunolol, were reduced to their active metabolites in mammals (20–23). Recently, Zhao *et al.* reported that RK is rapidly absorbed and metabolized in mice. They also found that the total bioavailability (AUC_{0-12h}) of RK and its metabolites, including ROH, as well as their accumulation in white adipose tissue, were higher in obese mice than in control mice when RK was administered orally (24). This suggests that the metabolism of RK, including its reduction, may differ depending on the pathophysiological stage of transition from non-obesity to obesity. These experimental results imply that the anti-obesity effect of RK may be an additive effect of ROH, as RK is easily eliminated by the mammalian body. However, no information currently exists on the reductive metabolism of RK in humans, taking it as a supplement, or on the anti-obesity effect of ROH. Therefore, it is important to examine unmetabolized RK as well as RK metabolism and the anti-obesity effects of its metabolites.

In this study, we clarified that RK is reductively metabolized to ROH in humans and investigated whether ROH and RK have anti-obesity effects in 3T3-L1 cells. We also investigated the effects of ROH on the expression of C/EBP α , PPAR γ , and adipogenesis-related genes.

Materials and methods

Chemicals. RK and isoproterenol were obtained from Tokyo Chemical Industry Co. Ltd. (Tokyo, Japan), and 3-Isobutyl-1-methylxanthine was purchased from FUJIFILM Wako Pure Chemical Co. (Tokyo, Japan). Insulin, dexamethasone, Dulbecco's modified Eagle's medium (DMEM), and a penicillin/streptomycin solution were purchased from Sigma-Aldrich (St. Louis, MO, USA). A glycerol assay kit (Cat. ab133130) was purchased from Abcam (Cambridge, UK). A pool of 150-donor mixed-gender human liver microsomes (Cat. 45215) and cytosol (Cat. 452117) was obtained from Corning Gentest (Corning, NY, USA). A CytoTox 96 non-radioactive cytotoxicity assay kit (Cat. G1780) was purchased from Promega (Madison, WI, USA). A lipid assay kit (Cat. AK09F) was purchased from Cosmo Bio Co. Ltd. (Tokyo, Japan). The reduced form of β -nicotinamide adenine dinucleotide phosphate (NADPH) was purchased from Oriental Yeast Co. Ltd. (Tokyo, Japan). HyClone™ fetal bovine serum (FBS) was purchased from Cytiva (Tokyo, Japan). Monoclonal antibodies against mouse C/EBP α (Cat. #8187) and horseradish peroxidase (HRP)-conjugated secondary antibodies were purchased from Cell Signaling Technology (Danvers, MA, USA). Monoclonal antibodies against mouse PPAR γ (Cat. sc-7273) were purchased from Santa Cruz Biotechnology Inc. (Dallas, TX, USA). HRP-conjugated anti-mouse β -actin antibody (Cat. A3854) was purchased from Sigma-Aldrich.

Procedure for synthesis of ROH. All commercial chemicals and solvents were of reagent grade and used without further purification. ROH was synthesized according to the method described by Kitayama *et al.* (25). A mixture of RK (12 mmol) and sodium borohydride (48 mmol) in methanol (50 ml) was stirred at 22°C for 3 h. The reaction progress was monitored by thin-layer chromatography (TLC) using commercially prepared silica gel 60 F₂₅₄ glass-backed plates.

After the solvent had evaporated, the residue was added to 10% hydrochloric acid (50 ml). The mixture was extracted three times with ethyl acetate (50 ml). The organic layer was washed with H₂O and brine, dried over anhydrous MgSO₄, and evaporated under reduced pressure. The residue was purified using column chromatography on silica gel (*n*-hexane/ethyl acetate). ROH was obtained as a white powder after recrystallization from *n*-hexane/ethyl acetate with a yield of 99%. The melting point of the purified ROH was determined using a Yanagimoto micromelting point apparatus (ANATEC YANACO Co., Kyoto, Japan). Infrared (IR) spectra were recorded using an FTIR-8400S spectrometer (Shimadzu Co., Kyoto, Japan). The ¹H nuclear magnetic resonance (¹H NMR) spectrum was obtained using a JNM-ECA500 spectrometer (JEOL Ltd., Tokyo, Japan). Proton chemical shifts were referenced to a tetramethylsilane internal standard. The *J* values are given in hertz. High-resolution mass spectrometry (HRMS) was performed using a JMS-T100GCv spectrometer (JEOL Ltd.). Elemental analysis was performed using a CE-440 CHN/O/S elemental analyzer (Exeter Analytical Inc., MA, USA), and the results were within $\pm 0.3\%$ of the theoretical values: m.p. 71–72°C. IR (KBr) cm⁻¹: 3350, 3036 (OH). ¹H NMR (500 MHz, CDCl₃-*d*) δ : 7.01 (d, 2H, *J*=8.6 Hz, ArH), 6.73 (d, 2H, *J*=8.6 Hz, ArH), 3.81 (m, 1H, -CH(OH)-), 2.97 (brs, 1H, -CH(OH)-), 2.60 (m, 2H, -CH₂CH₂-), 1.72 (m, 2H, -CH₂CH₂-), 1.21 (d, 3H, *J*=6.3 Hz, -CH₃). HRMS (EI) *m/z*: [M]⁺ Calcd for C₁₀H₁₄O₂ 166.0994; Found 166.0991. Anal. Calcd for C₁₀H₁₄O₂: C, 72.26; H, 8.49; O, 19.25. Found: C, 72.21; H, 8.58; O, 19.21.

Assay for RK-reductase activity. The reaction mixture consisted of 1.0 mM RK, 10 mM NADPH and 0.2 mg protein/ml human pooled liver microsomes or cytosol in 0.1 M potassium/sodium-phosphate buffer (pH 7.4) at a final volume of 2 ml. The reaction was performed at 37°C for 20 min. After incubation, the mixture was extracted twice with 5 ml ethyl acetate containing 1 μ M ethyl 4-hydroxybenzoate (an internal standard). The extraction mixture was centrifuged, and the organic layer was collected and evaporated to dryness. The residue was dissolved in 0.2 ml acetonitrile, and a 20 μ l sample was subjected to high-performance liquid chromatography (HPLC) analysis using a GL-7450 Hitachi chromatograph equipped with a CAPCELLPAK C8 UG120 column (Shiseido Co., Ltd., Tokyo, Japan) and 5 μ m (4.6x250 mm). The mobile phase was acetonitrile:0.1% acetic acid (3:7). The chromatograph was operated at a flow rate of 1 ml/min at 40°C, with detection at 280 nm. The amount of ROH formed was determined from the peak areas. The RK reductive activity was expressed as ROH nmol/min/mg protein.

3T3-L1 cell culture and differentiation. Mouse 3T3-L1 pre-adipocytes were obtained from the Japanese Collection of Research Resources Cell Bank (Osaka, Japan). The 3T3-L1 pre-adipocytes were cultured and maintained in DMEM containing 10% FBS, 100 U/ml penicillin, and 100 μ g/ml streptomycin (10% FBS-DMEM) (maintenance Medium; MM) at 37°C in 5% CO₂. The cells were seeded in 24-well plates at a density of 5x10⁴ cells/well and cultured in MM for 2 days until they reached semi-confluence. Differentiation to adipocytes was initiated by replacing the previous medium with MM containing 0.5 mM 3-isobutyl-1-methylxanthine,

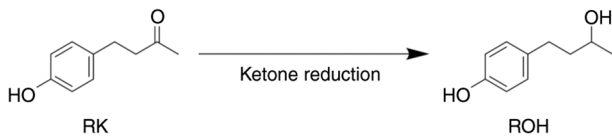


Figure 1. Reduction of RK in mammals. ROH, rhododendrol; RK, raspberry ketone.

1 μM dexamethasone, and 1 mg/ml insulin (differentiation medium; DM) (day 0) and incubating for 48 h (days 0-2). The DM was then replaced with MM containing 1 mg/ml insulin (adipocyte maintenance medium; AMM) and incubated for 48 h (days 2-4). The cells were then maintained, and the MM was replaced every 2 days until day 8 (days 4-8). The pre-adipocytes and adipocytes were incubated with DM, AMM, or MM in the absence or presence of ROH or RK (20-100 μM) from days 0 to 8. The cells differentiated by incubation with DM/AMM/MM without ROH or RK on day 8 were used as mature adipocytes.

Cell viability assay. The cytotoxic effects of ROH and RK on 3T3-L1 cells were estimated using a CytoTox 96 non-radioactive cytotoxicity assay kit. Briefly, cells were seeded in 24-well plates at a density of 5×10^4 cells/well. After 2 days, the cells were incubated with 10% FBS-DMEM in the absence or presence of ROH or RK (10-200 μM). After treatment for 24 h, lactate dehydrogenase (LDH) concentrations in the cell lysates were measured using the CytoTox 96 non-radioactive cytotoxicity assay kit following the manufacturer's instructions.

Oil Red O staining. Following differentiation, the culture medium was removed, and the cells were washed with phosphate buffered saline (-) [PBS (-)]. Oil Red O staining was performed using a lipid assay kit. Briefly, the cells were fixed with 10% formalin for 15 min at 22°C and then stained with Oil Red O-staining solution (60% isopropanol solution). This solution was prepared by diluting the Oil Red O stock solution to 60% with distilled water for 30 min at 22°C. The cells were washed with 60% isopropanol and distilled water. Images were captured using an Olympus IX71 inverted microscope (Olympus Co., Tokyo, Japan). The stained lipid droplets were dissolved in isopropanol and quantified by spectrophotometry at a wavelength of 540 nm.

Glycerol release assay. Mature 3T3-L1 adipocytes were incubated with DMEM containing 2% (w/v) fatty acid-free bovine serum albumin in the absence or presence of various concentrations of RK or ROH (20-100 μM). After incubation for 24 h, the culture medium was collected, and glycerol release activity was measured using a glycerol assay kit (Abcam PLC, Cambridge, UK) according to the manufacturer's instructions.

RNA isolation and quantitative polymerase chain reaction (qPCR). Total mRNA was isolated using ISOGEN II (Nippon Gene Co. Ltd., Tokyo, Japan) following the manufacturer's instructions. RNA was quantified using a Multiskan Sky High Microplate Spectrophotometer with a μdrop plate (Thermo Fisher Scientific Inc., Waltham, MA, USA), and 1 μg of RNA was reverse-transcribed using the ReverTra Ace

qPCR RT primary mix (Toyobo Co., Ltd., Osaka, Japan). PCR amplification of mouse leptin, C/EBP α , PPAR γ , and β -actin was performed using Thunderbird SYBR qPCR Mix (Toyobo Co., Ltd., Osaka, Japan) and a StepOne™ real-time PCR system (Thermo Fisher Scientific Inc., Waltham, MA, USA). The following thermocycling conditions for qPCR were used: initial denaturation at 95°C for 60 sec; and 40 cycles of denaturation at 95°C for 15 sec, and annealing/extension at 60°C for 60 sec. The primer sequences used for PCR were as follows: leptin forward 5'-CAGGATCAATGACATTTTCCACA CA-3'; leptin reverse 5'- GCTGGTGAGGACCTGTTGAT-3'; C/EBP α forward 5'-GCAGGAGGAAGATACAGGAAG-3'; C/EBP α reverse 5'-ACAGACTCAAATCCCCAACA-3'; PPAR γ forward 5'-GTGCTCCAGAAGATGACAGAC-3'; PPAR γ reverse 5'-GGTGGGACTTTCCTGCTAA-3'; β -actin forward 5'-TGGAACTCTGTGGCATCCATGAAAC-3', and β -actin reverse 5'-TAAAACGCAGCTCAGTAACAGTCC G-3'. C/EBP α and PPAR γ mRNA levels were calculated using the $2^{-\Delta\Delta C_q}$ method and normalized against the expression level of β -actin as an internal standard (26). All quantifications were performed independently three times.

Western blot analysis. The mature 3T3-L1 adipocytes were collected on day 8, washed twice with PBS (-), and lysed in radioimmunoprecipitation assay (RIPA) buffer (50 mM Tris-HCl, pH 8.0, 150 mM sodium chloride, 1% NP-40, 0.5% sodium deoxycholate, and 0.1% sodium dodecyl sulfate) containing protease inhibitor cocktail set I (FUJIFILM Wako Pure Chemical Co., Tokyo, Japan) on ice for 10 min. Cell lysates were centrifuged at 12,000 \times g for 15 min at 4°C. The supernatant was collected from the lysates and protein concentrations were determined using the bicinchoninic acid (BCA) method, with bovine serum albumin as the standard (27). Subsequently, 20 μg protein per lane was separated by 10% SDS-polyacrylamide gel electrophoresis and transferred to a polyvinylidene difluoride membrane (Millipore Sigma, Bedford, MA, USA). The membranes were incubated with Tris-buffered saline (20 mM Tris-HCl, pH 7.4, 150 mM sodium chloride) containing 0.05% Tween 20 and 2% skim milk as blocking solution for 2 h at 22°C. Membranes were then incubated with the indicated primary antibodies (mouse monoclonal anti-mouse C/EBP α , 1:2,000; rabbit monoclonal anti-mouse PPAR γ , 1:2,000; HRP-conjugated anti-mouse β -actin, 1:200,000) for 2 h at 22°C, further incubated with the HRP-conjugated secondary antibodies (1:5,000) for 1 h at 22°C and visualized using an enhanced ImmunoStar LD or ImmunoStar Zeta (both FUJIFILM Wako Pure Chemical Co.) with a LuminoGraph I (ATTO, Tokyo, Japan). Densitometric analysis was performed using the CS Analyzer 4 software (ATTO, Tokyo, Japan) and normalized against the expression level of β -actin as an internal standard.

Data analyses and statistics. All data are expressed as mean \pm standard deviation of the mean (SD). Statistical analyses were performed by using the unpaired Student's *t*-test or one-way ANOVA followed by Dunnett's post hoc test for multiple group comparisons. Calculations were performed using R (R Development Core Team). Statistical significance was set at $P < 0.05$.

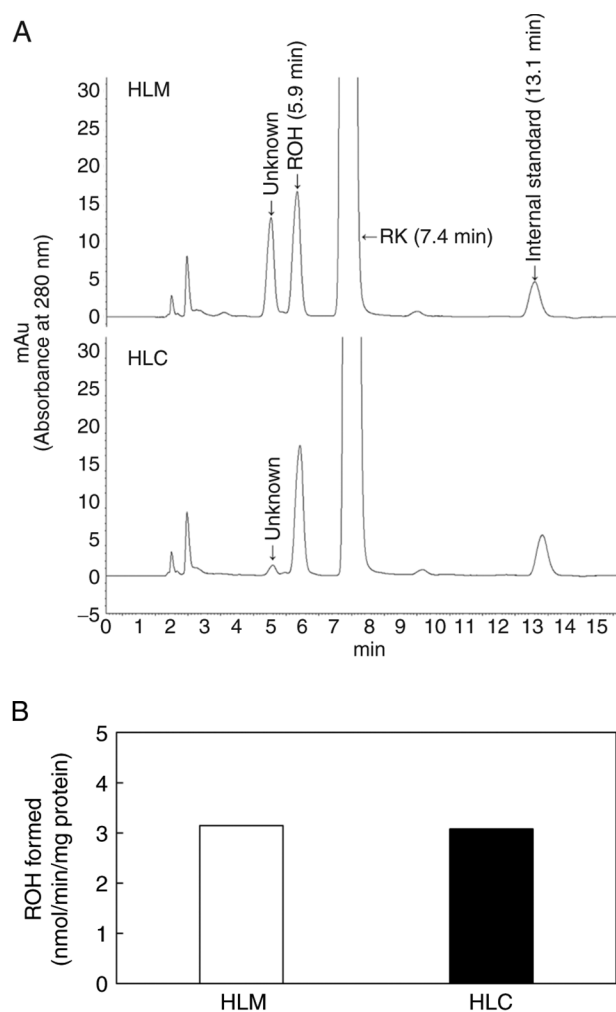


Figure 2. Identification of ROH by HPLC and reductase activity for RK to ROH in human liver microsomes or cytosol. RK (1.0 mM) and 10 mM NADPH were incubated with HLM or HLC in 0.1 M potassium/sodium-phosphate buffer (pH 7.4) at 37°C for 20 min. The compounds, including ROH, were extracted from the incubation mixture, as described in the *Materials and Methods*. (A) HPLC chromatograms obtained after incubation with HLM or HLC. (B) RK reduction activity in the presence of NADPH in HLMs and HLCs. The data presented are the means of duplicate experiments. HLC, human liver cytosol; HLM, human liver microsomes; ROH, rhododendrol; RK, raspberry ketone.

Results

RK reduction to ROH in human liver microsomes or cytosol.

To elucidate the metabolism of RK in humans, we examined the reduction of RK to ROH in human liver microsomes and cytosol. RK was incubated with human liver microsomes or the cytosol in the presence of NADPH. An HPLC chromatogram of the extract from the incubation mixtures containing liver microsomes revealed two peaks with retention times of 5.0 and 5.9 min, which differed from those of RK (7.4 min) and the internal standard (13.1 min). However, the peak at 5.0 min was slight in the incubation mixtures containing human liver cytosol (Fig. 2A). When RK was incubated with a cofactor and boiled human liver microsomes or cytosol, two peaks (5.0 and 5.9 min) were not detected (data not shown). The peak at 5.9 min, but not that at 5.0 min, was identified as ROH based on the retention time of the synthesized ROH (Fig. 2A). Both

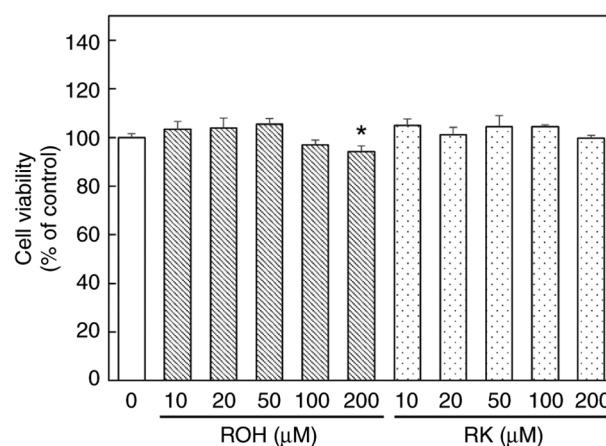


Figure 3. Effects of ROH and RK on cell viability. 3T3-L1 cells were treated with RK or ROH at various concentrations (10–200 μM), and cell viability was determined using a lactate dehydrogenase assay. Other details are described in the *Materials and Methods*. Each bar represents the mean ± standard deviation of three experiments. *P<0.05 vs. control. ROH, rhododendrol; RK, raspberry ketone.

the microsomes and cytosol showed RK reduction activity in the presence of NADPH (Fig. 2B). These results suggest that RK is reduced in humans as well as in other mammals.

Effects of ROH and RK on cell viability. The anti-adipogenic effect of RK at each maximum concentration of 10–300 μM has been determined (28–31). Here, 3T3-L1 cells were treated with various concentrations of ROH or RK (10–200 μM) for 24 h (Fig. 3) to evaluate cell viability. Cell viability at 24 h after treatment with 10–100 μM ROH or RK was similar to that of the untreated controls. However, treatment with 200 μM ROH resulted in only slight cytotoxicity. These results indicated that ROH or RK at concentrations up to 100 μM did not have a significant cytotoxic effect on these cells. Hence, all experiments were performed with ROH or RK at concentrations up to 100 μM.

Effects of ROH and RK on adipocyte differentiation in 3T3-L1 cells.

Leptin is predominantly expressed in adipose tissue and is considered an adipocyte marker protein (32,33). We measured leptin mRNA levels as adipocyte marker to confirm the formation of adipocytes from 3T3-L1 pre-adipocytes. Treatment of pre-adipocyte 3T3-L1 cells with DM/AMM/MM for 8 days significantly increased leptin mRNA levels compared with untreated pre-adipocytes (Fig. 4A). Therefore, we determined that pre-adipocyte 3T3-L1 cells were differentiated into mature adipocytes following DM/AMM/MM treatment for 8 days. The effects of ROH and RK on lipid accumulation during the differentiation of 3T3-L1 cells into adipocytes were compared. Oil Red O staining revealed that the addition of ROH (20–100 μM) to the culture medium during differentiation (days 0–8) decreased the number of lipid droplets in the cells in a dose-dependent manner, and had effects similar to those of RK (Fig. 4B). Moreover, the significant inhibitory effect of ROH, which was equivalent to that of RK, on lipid accumulation was confirmed by measuring Oil Red O levels in the cells (Fig. 4C). These results suggest that ROH, a metabolite of RK, is an active metabolite that can inhibit lipid droplet

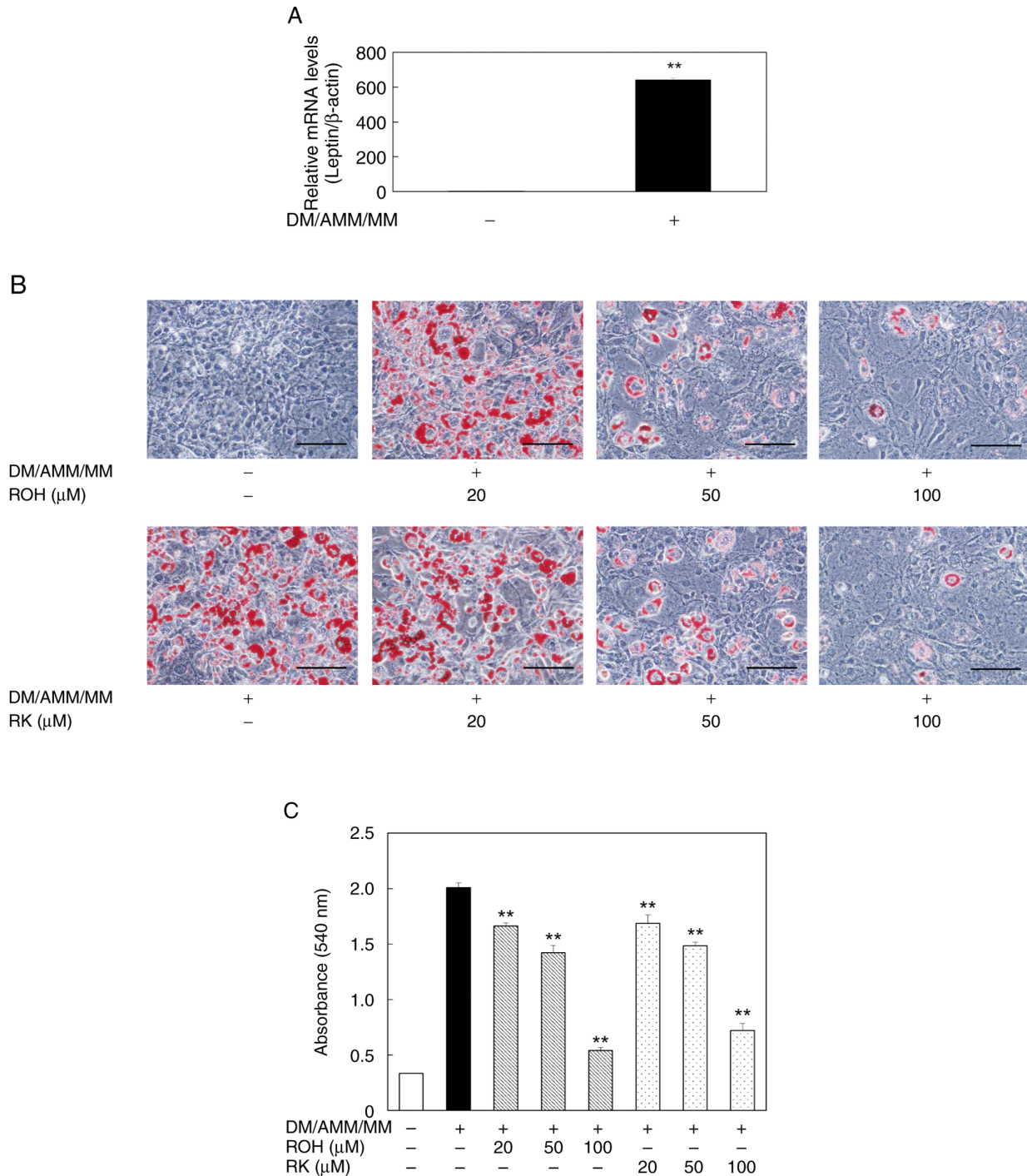


Figure 4. Effects of ROH and RK on lipid accumulation during differentiation of 3T3-L1 cells to adipocytes. (A) During differentiation of 3T3-L1, cells were treated with or without DM/AMM/MM for 8 days. Leptin mRNA levels in mature adipocytes (day 8) were examined by qPCR as an adipocyte marker. Each bar represents the mean \pm SD of three independent experiments. ** P <0.01 vs. without DM/AMM/MM. (B) During the differentiation of 3T3-L1, cells were treated with or without ROH or RK at various concentrations (20–100 μ M) for 8 days. Representative photomicrographs (magnification: \times 200, scale bar: 100 μ m) are shown for each treatment group. Oil Red O reagent-stained lipid droplets in the mature 3T3-L1 adipocytes (day 8). (C) The amount of lipid accumulated in mature 3T3-L1 adipocytes was quantified by measuring absorbance at 540 nm. Each bar represents the mean \pm SD of three independent experiments. ** P <0.01 vs. DM/AMM/MM alone. AMM, adipocyte maintenance medium; DM, differentiation medium; MM, maintenance medium; qPCR, quantitative PCR; ROH, rhododendrol; RK, raspberry ketone; SD, standard deviation.

accumulation in 3T3-L1 cells during their differentiation into adipocytes.

Effects of ROH and RK on glycerol release from mature 3T3-L1 adipocytes. We examined the release of glycerol

into the culture medium after treatment with ROH or RK (20–100 μ M) for 24 h to assess whether ROH promoted lipolysis in mature 3T3-L1 adipocytes. Treatment of the cells with 50 μ M ROH, 100 μ M ROH, or RK increased glycerol release into the medium by 1.18-fold, 1.44-fold

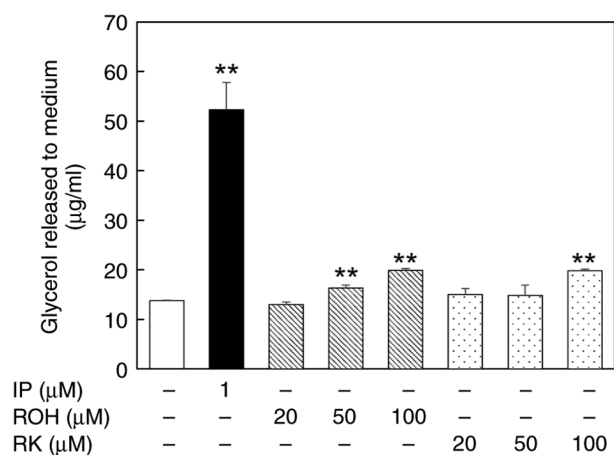


Figure 5. Effects of ROH and RK on mature 3T3-L1 adipocytes glycerol-release activity. Mature 3T3-L1 adipocytes (day 8) were treated with or without ROH or RK at various concentrations (20-100 μ M) for 24 h. Glycerol-release activity was quantified by measuring the absorbance at 540 nm. Each bar represents the mean \pm standard deviation of three experiments. ** $P < 0.01$ vs. control. IP; isoproterenol; ROH, rhododendrol; RK, raspberry ketone.

and 1.43-fold, respectively, compared with untreated cells (Fig. 5). Therefore, ROH shows a lipolysis-promoting effect, similar to that of RK.

Effects of ROH and RK on C/EBP α and PPAR γ mRNA and protein levels in 3T3-L1 adipocytes. As ROH showed an inhibitory effect on lipid accumulation, we focused on how it might affect the regulation of the expression of adipogenesis-related genes such as C/EBP α and PPAR γ . The effects of ROH on C/EBP α and PPAR γ mRNA levels in mature adipocytes were investigated and compared with those of RK. When 3T3-L1 pre-adipocytes were treated with ROH (20-100 μ M) during their differentiation into adipocytes over 8 days, C/EBP α and PPAR γ mRNA levels decreased in a concentration-dependent manner. Treatment with RK produced similar results (Figs. 6A and B). Furthermore, the expression levels of C/EBP α and PPAR γ proteins were monitored using western blot analysis (Fig. 7A). The treatment of the pre-adipocyte 3T3-L1 cells with ROH and RK (20-100 μ M) during differentiation downregulated PPAR γ protein expression in mature 3T3-L1 adipocytes on day 8 in a concentration-dependent manner (Fig. 7C). However, the levels of C/EBP α protein remained unchanged (Fig. 7B). The anti-adipogenic effects of ROH and RK may be attributed to their PPAR γ lowering effects; however, it remains unclear as to why the lowering effects of ROH and RK on C/EBP α mRNA levels were not reflected in their protein levels.

Discussion

This study demonstrated that RK was reduced to ROH in human liver microsomes and cytosol. Because the reduction of RK occurs in both human liver microsomes and the cytosol in the presence of NADPH, and other carbonyl compounds, such as warfarin and nabumetone, are also metabolized in this manner, multiple enzymes are thought to be involved in this reaction (34,35). Additionally, our data showed a new peak for the RK metabolite with a retention time of 5.0 min

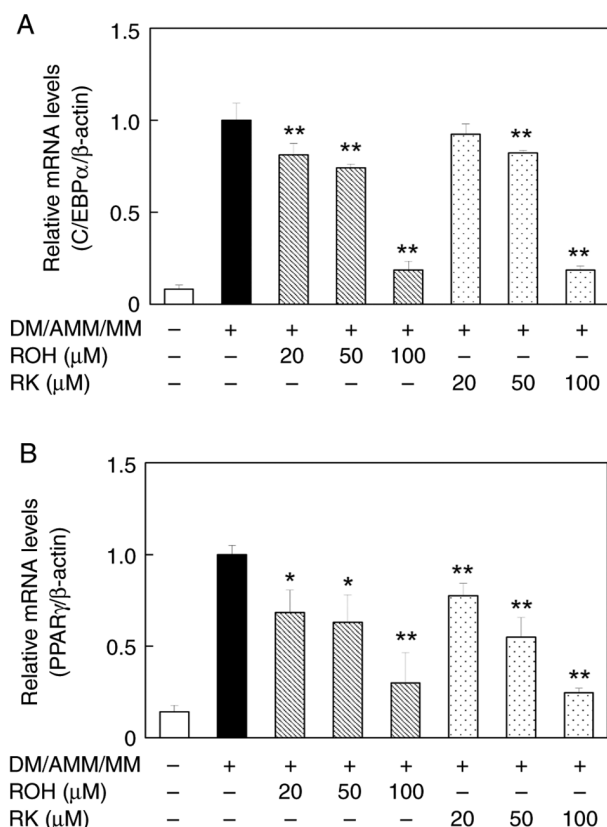


Figure 6. Effects of ROH and RK on the mRNA levels of adipogenesis-related genes in adipocyte differentiation. Various concentrations (20-100 μ M) of ROH or RK were added to 3T3-L1 pre-adipocytes for 8 days. (A) C/EBP α and (B) PPAR γ mRNA levels in mature adipocytes (day 8) were examined using quantitative PCR. Each bar represents the mean \pm standard deviation of three independent experiments. * $P < 0.05$, ** $P < 0.01$ vs. DM/AMM/MM alone. AMM, adipocyte maintenance medium; C/EBP α , CCAAT enhancer-binding protein α ; DM, differentiation medium; MM, maintenance medium; PPAR γ , peroxisome proliferator-activated receptor γ ; ROH, rhododendrol; RK, raspberry ketone.

after incubation with human liver microsomes. In addition to ROH, the metabolites of RK include 4-(3,4-Dihydroxyphenyl) butanone, which is generated by the hydroxylation of RK, and 4-(2-Hydroxyethyl) phenol (tyrosol), which is generated by decarboxylation of ROH (24). However, when ROH was incubated with human liver microsomes in the presence of NADPH, no unknown metabolites were detected, with a retention time of 5 min (data not shown). Therefore, the metabolite with a retention time of 5 min in the chromatogram was not 4-(2-hydroxyethyl) phenol (tyrosol). We are also interested in metabolites other than ROH, and further studies should focus on the metabolic mechanisms that produce these molecules and how they affect the suppression of fat accumulation.

RK and various other compounds suppress the differentiation of 3T3-L1 cells into adipocytes (7,8,30,31). Our data revealed that RK suppressed the lipid accumulation-induced differentiation of 3T3-L1 pre-adipocytes in a dose-dependent manner, which is consistent with previous reports. In addition, this study showed that ROH, a reductive metabolite of RK, suppressed lipid accumulation during the differentiation of pre-adipocytes into adipocytes, suggesting that ROH is an active metabolite. Recently, a pharmacokinetic study of orally administered RK demonstrated that the accumulation of RK and its metabolites

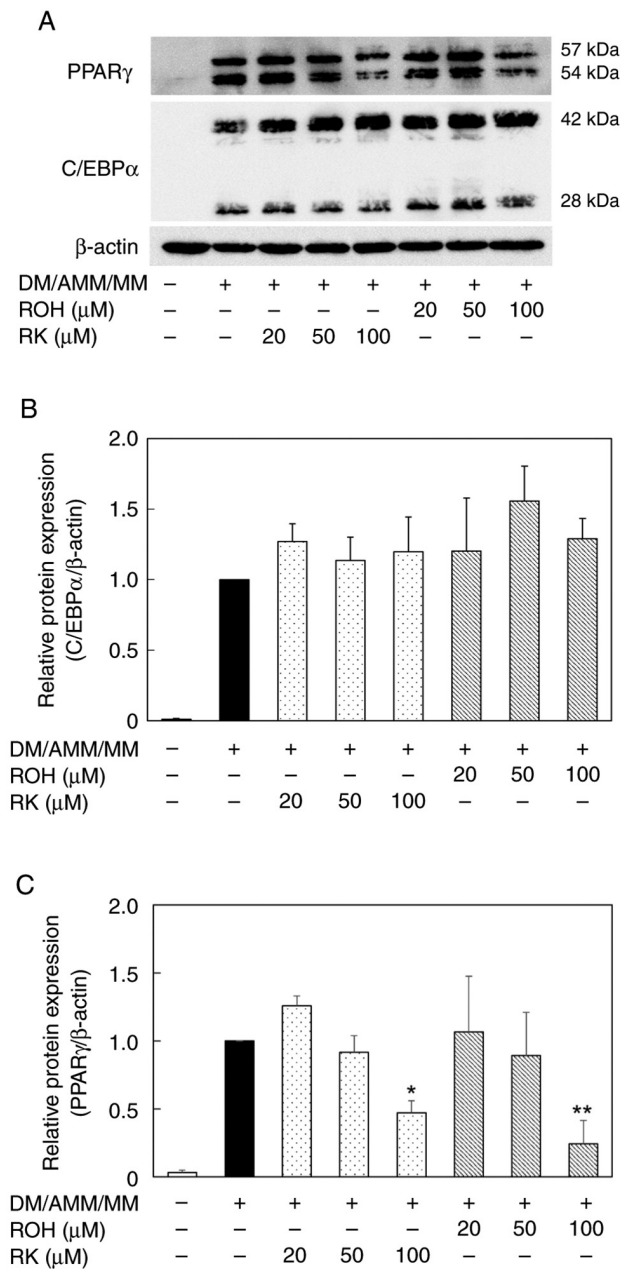


Figure 7. Effects of ROH and RK on the protein expression of adipogenic transcription factor in adipocyte differentiation. Various concentrations (20-100 μM) of ROH or RK were added to 3T3-L1 pre-adipocytes for 8 days. (A) C/EBPα and PPARγ protein expression in mature adipocytes (day 8) was examined by western blot analysis. Quantification of the protein expression of (B) C/EBPα and (C) PPARγ. Each bar represents the mean ± standard deviation of three independent experiments. *P<0.05, **P<0.01 vs. DM/AMM/MM alone. AMM, adipocyte maintenance medium; C/EBPα, CCAAT enhancer-binding protein α; DM, differentiation medium; MM, maintenance medium; PPARγ, peroxisome proliferator-activated receptor γ; ROH, rhododendrol; RK, raspberry ketone.

in the white adipose tissue of obese mice was higher than that in normal mice (24). Therefore, ROH produced when RK is orally administered during the development of obesity may act additively with RK in pre-adipose and adipose tissues to produce anti-obesity effects. A dietary supplement mixture containing RK, capsaicin, caffeine, garlic, and Citrus aurantium reduced the body weight and fat in overweight adults (36), but there is no information on their effects after oral administration of RK

alone to human or human adipocytes. The present study will be a useful basis for investigating the anti-obesity effects ROH and RK in humans. Studies of foods containing active ingredients with anti-obesity effects, such as health foods and supplements, have examined the ingredients that are ingested. The results of this study suggest that metabolites produced after oral ingestion may also exhibit anti-adipogenic and lipolysis-promoting activities. Our findings may aid in the development of more effective anti-obesity drugs and the prevention of visceral fatty obesity and fatty liver disease.

The regulation of the expression of adipogenesis-related factors, including C/EBPα and PPARγ, contributes to the differentiation of pre-adipocytes into adipocytes (4,5). Regulation of C/EBPα and PPARγ gene expression is involved in adipogenesis, and their downregulation is related to adipogenesis suppression (37). In addition, activation (phosphorylation) of AMP-activated protein kinase (AMPK), which exerts anti-obesity effects via regulation of the expression and activation of enzymes involved in lipid metabolism, is a critical event in lipolysis (38,39). Previous studies have demonstrated that several natural flavonoids suppress adipogenesis by activating AMPK and downregulating the C/EBPα and PPARγ genes (40,41). The suppressive effect of RK on 3T3-L1 cell differentiation into adipocytes seemed to be caused by the downregulation of the mRNA levels of C/EBPα and PPARγ. In the present study, we also found that, similar to RK, ROH suppressed the differentiation of cells and decreased the mRNA levels of C/EBPα and PPARγ and protein expression of PPARγ, but not C/EBPα protein. Our data suggest that the downregulation of PPARγ by ROH and RK contributed to their anti-adipogenic effects. PPARγ plays an important role in adipose differentiation through the regulation of the expression of adipocyte-specific genes, such as adipocyte fatty acid-binding protein-2 (aP2) and fatty acid synthase (FASN) (42). The ROH- or RK-suppressed PPARγ expression may affect the regulation of their adipocyte-related genes. Further study remains on the effects of ROH and RK against the genes regulated by PPARγ.

Park demonstrated that RK has a lipolysis-promoting effect on glycerol release from 3T3-L1 adipocytes (30). Our data support this finding and suggest that ROH has a lipolysis-promoting effect similar to that of RK. Therefore, the suppressive effects of ROH and RK on 3T3-L1 cell differentiation into adipocytes may be caused by the downregulation of mRNA and protein expression of adipogenesis-related factors and lipolysis. If lipolysis is not involved, glycerol released from the cells may have a similar effect. Further studies are required to elucidate the mechanisms by which ROH and RK promote lipolysis.

The chemical structure of RK is similar to those of capsaicin, 6-gingerol, and synephrine, which are the principal components of hot red pepper, ginger, and citrus plants, respectively. These compounds have been shown to suppress lipid accumulation (43-45). The anti-adipogenic effects of ROH and RK may be due to their structural similarities to these compounds. Whether there exists a structure-activity relationship that contributes to the anti-obesity effects of RK, capsaicin, 6-gingerol, synephrine, and their metabolites is of considerable interest; studies to determine this are now underway.

In conclusion, we showed that ROH, a reductive metabolite of RK, has an anti-adipogenic effect similar to that of RK in the differentiation of 3T3-L1 cells into adipocytes. These results imply that both RK and ROH might contribute to the anti-obesity effects of orally ingested RK. Our results suggest that the biological effects of natural compounds, including their anti-obesity effects, may be due to their metabolites. Therefore, we propose that it is important to evaluate the biological activity of all detectable metabolites and consider their pharmacokinetics.

Acknowledgements

Not applicable.

Funding

This work was supported in part by JSPS KAKENHI (grant no. JP21K11599).

Availability of data and materials

The datasets used and/or analyzed during the current study are available from the corresponding author upon reasonable request.

Authors' contributions

NU and TH contributed to experimental design. NU, AK, MO and TH performed the experiments. NU, MO and TH wrote the manuscript. NU, AK, MO and TH confirm the authenticity of all raw data. All authors read and approved the final manuscript.

Ethics approval and consent to participate

Not applicable.

Patient consent for publication

Not applicable.

Competing interests

The authors declare that they have no competing interests.

References

- Ding J, Reynolds LM, Zeller T, Müller C, Lohman K, Nicklas BJ, Kritchevsky SB, Huang Z, de la Fuente A, Soranzo N, *et al*: Alterations of a cellular cholesterol metabolism network are a molecular feature of obesity-related type 2 diabetes and cardiovascular disease. *Diabetes* 64: 3464-3474, 2015.
- Kopelman PG: Obesity as a medical problem. *Nature* 404: 635-643, 2000.
- Garg SK, Maurer H, Reed K and Selagamsetty R: Diabetes and cancer: Two diseases with obesity as a common risk factor. *Diabetes Obes Metab* 16: 97-110, 2014.
- Cao Z, Umek RM and McKnight SL: Regulated expression of three C/EBP isoforms during adipose conversion of 3T3-L1 cells. *Genes Dev* 5: 1538-1552, 1991.
- Farmer SR: Transcriptional control of adipocyte formation. *Cell Metab* 4: 263-273, 2006.
- Morrison S and McGee SL: 3T3-L1 adipocytes display phenotypic characteristics of multiple adipocyte lineages. *Adipocyte* 4: 295-302, 2015.
- Kim EJ, Kang MJ, Seo YB, Nam SW and Kim GD: Acer okamotoanum Nakai leaf extract inhibits adipogenesis via suppressing expression of PPAR γ and C/EBP α in 3T3-L1 cells. *J Microbiol Biotechnol* 28: 1645-1653, 2018.
- Lee MS, Kim CT, Kim IH and Kim Y: Inhibitory effects of green tea catechin on the lipid accumulation in 3T3-L1 adipocytes. *Phytother Res* 23: 1088-1091, 2009.
- Gallois A: Quantitative evaluation of raspberry ketone using thin-layer chromatography. *Sci Aliments* 2: 99-106, 1982.
- Larsen M, Poll L, Callesen O and Lewis M: Relations between the content of aroma compounds and the sensory evaluation of 10 raspberry varieties (*Rubus idaeus* L). *Acta Agric Scand* 41: 447-454, 1991.
- Mehanna ET, Barakat BM, El Sayed MH and Tawfik MK: An optimized dose of raspberry ketone controls hyperlipidemia and insulin resistance in male obese rats; Effect on adipose tissue expression of adipocytokines and aquaporin 7. *Eur J Pharmacol* 832: 81-89, 2018.
- Wang L, Meng X and Zhang F: Raspberry ketone protects rats fed high-fat diets against nonalcoholic steatohepatitis. *J Med Food* 15: 495-503, 2012.
- Morimoto C, Satoh Y, Hara M, Inoue S, Tsujita T and Okuda H: Anti-obese action of raspberry ketone. *Life Sci* 77: 194-204, 2005.
- Fuchino H, Konishi S, Satoh T, Yagi A, Saitsu K, Tatsumi T and Tanaka N: Chemical evaluation of *Betula* species in Japan. II. Constituents of *Betula platyphylla* var *japonica*. *Chem Pharm Bull* 44: 1033-1038, 1996.
- Inoue T, Ishidate Y, Fujita M, Kubo M, Fukushima M and Nagai M: Studies on the constituents of *Aceraceae* plants. I. Constituents in the leaves and the stem bark of *Acer nikoense* Maxim (author's transl). *Yakugaku Zasshi* 98: 41-46, 1978 (In Japanese).
- Li X, Wei T, Wu M, Chen F, Zhang P, Deng ZY and Luo T: Potential metabolic activities of raspberry ketone. *J Food Biochem* 46: e14018, 2022.
- Sporstøl S and Scheline RR: The metabolism of 4-(4-hydroxyphenyl)butan-2-one (raspberry ketone) in rats, guinea-pigs and rabbits. *Xenobiotica* 12: 249-257, 1982.
- Tanaka Y, Nishikawa Y, Matsuda K, Yamazaki M and Hayashi R: Purification and some properties of ketone reductase forming an active metabolite of sodium 2-[4-(2-oxocyclopentyl methyl)-phenyl]propionate dihydrate (loxoprofen sodium), a new anti-inflammatory agent, in rabbit liver cytosol. *Chem Pharm Bull (Tokyo)* 32: 1040-1048, 1984.
- Sasaki K, Yamauchi K and Kuwano S: Metabolic activation of sennoside A in mice. *Planta Med* 37: 370-378, 1979.
- Murata H, Higuchi T and Otagiri M: Oral pharmacokinetics and in-vitro metabolism of metyrapone in male rats. *J Pharm Pharmacol* 68: 970-979, 2016.
- Imamura Y, Iwamoto K, Yanachi Y, Higuchi T and Otagiri M: Postnatal development, sex-related difference and hormonal regulation of acetoheamide reductase activities in rat liver and kidney. *J Pharmacol Exp Ther* 264: 166-171, 1993.
- Higuchi T, Imamura Y and Otagiri M: Kinetic studies on the reduction of acetoheamide catalyzed by carbonyl reductase from rabbit kidney. *Biochim Biophys Acta* 1158: 23-28, 1993.
- Imamura Y, Nozaki Y, Higuchi T and Otagiri M: Reactivity for prostaglandins and inhibition by nonsteroidal anti-inflammatory drugs of rabbit liver Bufenolol reductase. *Res Commun Chem Pathol Pharmacol* 71: 49-57, 1991.
- Zhao D, Yuan B, Kshatriya D, Polyak A, Simon JE, Bello NT and Wu Q: Influence of diet-induced obesity on the bioavailability and metabolism of raspberry ketone (4-(4-hydroxyphenyl)-2-butanone) in mice. *Mol Nutr Food Res* 64: e1900907, 2020.
- Kitayama T, Isomori S and Nakamura K: Asymmetric synthesis of enantiomerically pure zingerols by lipase-catalyzed transesterification and efficient synthesis of their analogues. *Tetrahedron Asymmetry* 24: 621-627, 2013.
- Livak KJ and Schmittgen TD: Analysis of relative gene expression data using real-time quantitative PCR and the 2(-Delta Delta C(T)) method. *Methods* 25: 402-408, 2001.
- Smith PK, Krohn RI, Hermanson GT, Mallia AK, Gartner FH, Provenzano MD, Fujimoto EK, Goeke NM, Olson BJ and Klenk DC: Measurement of protein using bicinchoninic acid. *Anal Biochem* 150: 76-85, 1985.
- Leu SY, Chen YC, Tsai YC, Hung YW, Hsu CH, Lee YM and Cheng PY: Raspberry ketone reduced lipid accumulation in 3T3-L1 cells and ovariectomy-induced obesity in Wistar rats by regulating autophagy mechanisms. *J Agric Food Chem* 65: 10907-10914, 2017.

29. Tsai YC, Chen JH, Lee YM, Yen MH and Cheng PY: Raspberry ketone promotes FNDC5 protein expression via HO-1 upregulation in 3T3-L1 adipocytes. *Chin J Physiol* 65: 80-86, 2022.
30. Park KS: Raspberry ketone increases both lipolysis and fatty acid oxidation in 3T3-L1 adipocytes. *Planta Med* 76: 1654-1658, 2010.
31. Park KS: Raspberry ketone, a naturally occurring phenolic compound, inhibits adipogenic and lipogenic gene expression in 3T3-L1 adipocytes. *Pharm Biol* 53: 870-875, 2015.
32. Zhang Y, Proenca R, Maffei M, Barone M, Leopold L and Friedman JM: Positional cloning of the mouse obese gene and its human homologue. *Nature* 372: 425-432, 1994.
33. Halaas JL, Gajiwala KS, Maffei M, Cohen SL, Chait BT, Rabinowitz D, Lallone RL, Burley SK and Friedman JM: Weight-reducing effects of the plasma protein encoded by the obese gene. *Science* 269: 543-546, 1995.
34. Malátková P, Sokolová S, Chocholoušová Havlíková LC and Wsól V: Carbonyl reduction of warfarin: Identification and characterization of human warfarin reductases. *Biochem Pharmacol* 109: 83-90, 2016.
35. Matsumoto K, Hasegawa T, Koyanagi J, Takahashi T, Akimoto M and Sugibayashi K: Reductive metabolism of nabumetone by human liver microsomal and cytosolic fractions: Exploratory prediction using inhibitors and substrates as marker probes. *Eur J Drug Metab Pharmacokinet* 40: 127-135, 2015.
36. Arent SM, Walker AJ, Pellegrino JK, Sanders DJ, McFadden BA, Ziegenfuss TN and Lopez HL: The combined effects of exercise, diet, and a multi-ingredient dietary supplement on body composition and adipokine changes in overweight Adults. *J Am Coll Nutr* 37: 111-120, 2018.
37. White UA and Stephens JM: Transcriptional factors that promote formation of white adipose tissue. *Mol Cell Endocrinol* 318: 10-14, 2010.
38. Zhang BB, Zhou G and Li C: AMPK: An emerging drug target for diabetes and the metabolic syndrome. *Cell Metab* 9: 407-416, 2009.
39. Ceddia RB: The role of AMP-activated protein kinase in regulating white adipose tissue metabolism. *Mol Cell Endocrinol* 366: 194-203, 2013.
40. Piao GC, Liu GC, Jin XJ, Jin D and Yuan HD: Tetrahydropalmitine inhibits lipid accumulation through AMPK signaling pathway in 3T3-L1 adipocytes. *Mol Med Rep* 15: 3912-3918, 2017.
41. Wang G, Wu B, Xu W, Jin X, Wang K and Wang H: The inhibitory effects of Juglanin on adipogenesis in 3T3-L1 adipocytes. *Drug Des Dev Ther* 14: 5349-5357, 2020.
42. Jefcoate CR, Wang S and Liu X: Methods that resolve different contributions of clonal expansion to adipogenesis in 3T3-L1 and C3H10T1/2 cells. *Methods Mol Biol* 456: 173-193, 2008.
43. Lee MS, Kim CT, Kim IH and Kim Y: Effects of capsaicin on lipid catabolism in 3T3-L1 adipocytes. *Phytother Res* 25: 935-939, 2011.
44. Tzeng TF and Liu IM: 6-gingerol prevents adipogenesis and the accumulation of cytoplasmic lipid droplets in 3T3-L1 cells. *Phytomedicine* 20: 481-487, 2013.
45. Guo LX, Chen G, Yin ZY, Zhang YH and Zheng XX: p-Synephrine exhibits anti-adipogenic activity by activating the Akt/GSK3 β signaling pathway in 3T3-L1 adipocytes. *J Food Biochem* 43: e13033, 2019.



This work is licensed under a Creative Commons Attribution-NonCommercial-NoDerivatives 4.0 International (CC BY-NC-ND 4.0) License.